ISTANBUL TECHNICAL UNIVERSITY ★ GRADUATE SCHOOL OF SCIENCE ENGINEERING AND TECHNOLOGY

A FOURIER PSEUDO-SPECTRAL METHOD FOR THE HIGHER-ORDER BOUSSINESQ EQUATION

M.Sc. THESIS

Göksu TOPKARCI

Department of Mathematical Engineering

Mathematical Engineering Programme

JANUARY 2015

ISTANBUL TECHNICAL UNIVERSITY ★ GRADUATE SCHOOL OF SCIENCE ENGINEERING AND TECHNOLOGY

A FOURIER PSEUDO-SPECTRAL METHOD FOR THE HIGHER-ORDER BOUSSINESQ EQUATION

M.Sc. THESIS

Göksu TOPKARCI
(509121058)

Department of Mathematical Engineering

Mathematical Engineering Programme

Thesis Advisor: Assoc. Prof. Dr. Gülçin Mihriye MUSLU

JANUARY 2015

İSTANBUL TEKNİK ÜNİVERSİTESİ ★ FEN BİLİMLERİ ENSTİTÜSÜ

YÜKSEK MERTEBEDEN BOUSSINESQ DENKLEMİ İÇİN FOURIER SPEKTRAL YÖNTEMİ

YÜKSEK LİSANS TEZİ

Göksu TOPKARCI
(509121058)

Matematik Mühendisliği Anabilim Dalı

Matematik Mühendisliği Programı

Tez Danışmanı: Assoc. Prof. Dr. Gülçin Mihriye MUSLU

OCAK 2015

Göksu TOPKARCI, a M.Sc. student of ITU Graduate School of Science Engineering and Technology 509121058 successfully defended the thesis entitled **"A FOURIER PSEUDO-SPECTRAL METHOD FOR THE HIGHER-ORDER BOUSSINESQ EQUATION"**, which he/she prepared after fulfilling the requirements specified in the associated legislations, before the jury whose signatures are below.

Thesis Advisor :	**Assoc. Prof. Dr. Gülçin Mihriye MUSLU** Istanbul Technical University	.....
Co-advisor :	**Assist. Prof. Dr. Handan BORLUK** Kemerburgaz University	.....
Jury Members :	**Prof. Dr. Albert Kohen Erkip** Sabancı University	.....
	Assoc. Prof. Dr. Ceni BABAOĞLU İstanbul Tecnhical University	.....
	Assist. Prof. Dr. Ahmet KIRIŞ İstanbul Tecnhical University	.....

Date of Submission : **15 December 2014**
Date of Defense : **23 January 2015**

To my family,

FOREWORD

I would like to express my deep appreciation and thanks to my advisor Assoc. Prof. Dr. Gülçin Mihriye Muslu and my co-advisor Assist. Prof. Dr. Handan Borluk for their indispensable support and for spending their valuable time and knowledge.
Secondly, I want to give an acknowledgement to Res. Assist. Gökhan Göksu for helping me in LaTeX and MATLAB. I want to show my gratefulness to my mother Necla Topkarcı, my father Ömer Topkarcı , my brother Asım Topkarcı and Yakup Oruç for their infinite support.
This thesis study has been supported by the Scientific and Technological Research Council of Turkey (TUBITAK) under the project MFAG-113F114.

January 2015

Göksu TOPKARCI
(Research Assistant)

TABLE OF CONTENTS

Page

FOREWORD ..... **ix**
TABLE OF CONTENTS ..... **xi**
LIST OF TABLES ..... **xiii**
LIST OF FIGURES ..... **xv**
SUMMARY ..... **xvii**
ÖZET ..... **xix**
1. THE FOURIER SYSTEM **1**
1.1 Introduction 1
1.2 Preliminaries 1
1.3 Continuous Fourier Expansion 3
1.4 Discrete Fourier Expansion 6
1.5 Differentiation in Spectral Methods 10
2. THE HIGHER-ORDER BOUSSINESQ EQUATION **13**
2.1 Introduction 13
2.2 The Higher-Order Boussinesq Equation 13
2.3 Solitary Wave Solution 14
3. THE PSEUDO-SPECTRAL METHOD FOR THE HIGHER-ORDER BOUSSINESQ EQUATION **17**
3.1 Introduction 17
3.2 The Semi-Discrete Scheme 17
3.2.1 Convergence of the semi-discrete scheme 18
3.3 The Fully-Discrete Scheme 21
3.4 Numerical Experiments 23
3.4.1 Propagation of a Single Solitary Wave 24
3.4.2 Head-on Collision of Two Solitary Waves 26
3.4.3 Blow-up 29
3.4.4 Conclusion 32
REFERENCES **33**
CURRICULUM VITAE **35**

LIST OF TABLES

Page

Table 3.1 : The convergence rates in time calculated from the L_∞-errors in the case of single solitary wave ($A \approx 0.39,\ N = 512$) 25

Table 3.2 : The convergence rates in space calculated from the L_∞-errors in the case of the single solitary wave ($A \approx 0.39,\ M = 1000$)..... 25

LIST OF FIGURES

Page

Figure 1.1 : Comparison $P_N u$, $I_N u$ and exact solution $u(x)$ for $N = 16$ 8
Figure 1.2 : Comparison $P_N u$, $I_N u$ and exact solution $u(x)$ for $N = 32$ 8
Figure 1.3 : Comparison $P_N u$, $I_N u$ and exact solution $u(x)$ for $N = 8$ 9
Figure 1.4 : Comparison $P_N u$, $I_N u$ and exact solution $u(x)$ for $N = 16$ 9
Figure 1.5 : Comparison $P_N u$, $I_N u$ and exact solution $u(x)$ for $N = 32$ 10
Figure 1.6 : $P_N u'$, $(I_N u)'$, $I_N u'$ and $u'(x)$ for $N = 8$ 11
Figure 1.7 : $P_N u'$, $(I_N u)'$, $I_N u'$ and $u'(x)$ for $N = 16$ 12
Figure 1.8 : $P_N u'$, $(I_N u)'$, $I_N u'$ and $u'(x)$ for $N = 32$ 12
Figure 3.1 : L_∞-errors for the increasing values of N 24
Figure 3.2 : Head-on collision of two solitary waves with amplitude $A \approx 0.39$ ... 27
Figure 3.3 : Evolution of the change in the conserved quantity mass 27
Figure 3.4 : Head-on collision of two solitary waves with amplitude $A \approx 1.08$ ... 28
Figure 3.5 : Evolution of the change in the conserved quantity mass 28
Figure 3.6 : The variation of $\| U \|_\infty$ with time 30
Figure 3.7 : The variation of $\| U \|_\infty$ with time 30
Figure 3.8 : The variation of $\| U \|_\infty$ with time 31
Figure 3.9 : The variation of $\| U \|_\infty$ with time 32

A FOURIER PSEUDO-SPECTRAL METHOD FOR THE HIGHER-ORDER BOUSSINESQ EQUATION

SUMMARY

The higher-order Boussinesq equation (HBq) is given by

$$u_{tt} = u_{xx} + \eta_1 u_{xxtt} - \eta_2 u_{xxxxtt} + (f(u))_{xx}$$

where $f(u) = u^p$ and $p > 1$ is an integer. Here η_1 and η_2 are real positive constants. The HBq equation models the longitudinal vibrations of a dense lattice. In this thesis study, we propose a Fourier pseudo-spectral method for the HBq equation.

The Thesis is organized as follows:

Chapter 1 is devoted to the preliminaries. We briefly review some basic definitions related to linear algebra, some special function spaces and weak derivative. We also introduce continuous and discrete Fourier transforms. We then consider three examples to understand discrete and continuous Fourier expansions and differentiation.

In Chapter 2, we first give a brief introduction to the HBq equation and its properties such as conserved quantities. We then derive solitary wave solutions of the HBq equation by using the ansatz method which is one of the most effective direct methods to construct the solitary wave solutions of the nonlinear evolution equation.

In Chapter 3, we introduce the Fourier pseudo-spectral method for the HBq equation. We first prove the convergence of the semi-discrete scheme in the appropriate energy space. We then define fully-discrete scheme for the HBq equation. Solution steps are *(i)* constituting the grid points in space, *(ii)* transforming the equation into the Fourier space and obtaining an ordinary differential equation in terms of Fourier coefficients, *(iii)* solving the resulting ordinary differential equation by using the fourth-order Runge-Kutta method (RK4), iv) forming the numerical solution from Fourier coefficients by using the inverse Fourier transform. To see the validation of the proposed scheme, we consider three test problems concerning the propagation of a single solitary wave, the interaction of two solitary waves and a solution that blows up in finite time. In these problems, we consider various power type nonlinearities. Our numerical results show that the Fourier pseudo-spectral method exhibits fourth-order convergence in time and provides spectral accuracy in space. As far as we know, the present study is the first numerical study in the literature for the HBq equation. Therefore, we could not compare our numerical results with the results in the literature.

YÜKSEK MERTEBEDEN BOUSSINESQ DENKLEMİ İÇİN FOURIER SPEKTRAL YÖNTEMİ

ÖZET

Yüksek mertebeden Boussinesq denklemi (HBq)

$$u_{tt} = u_{xx} + \eta_1 u_{xxtt} - \eta_2 u_{xxxxtt} + (f(u))_{xx}$$

ile verilmektedir. Burada doğrusal olmayan terim $f(u) = u^p, \quad p > 1$ bir tamsayı olup, η_1 ve η_2 pozitif gerçel değerli parametrelerdir. Denklemdeki x ve t sırasıyla uzaysal ve zamansal değişkenleri temsil etmektedir. Yüksek mertebeden Boussinesq denklemi ilk olarak Rosenau tarafından türetilmiştir. Daha sonra bu denklem Duruk ve diğerleri tarafından sonsuz elastik bir ortamda doğrusal ve yerel olmayan özellikteki boyuna dalgaların yayılımını modellemek için tekrar türetilmiştir. HBq denklemindeki terimlere ek olarak u_{xxxx} doğrusal terimini içeren bir denklem ise Schneider ve Wayne tarafından yüzey gerilimli su dalgalarını modellemek üzere türetilmiştir. Yerel ve doğrusal olmayan dalga denklemi

$$u_{tt} = (\beta * (u + g(u)))_{xx}$$

çekirdek fonksiyonunun Fourier transformunun

$$\widehat{\beta}(\xi) = \frac{1}{1 + \eta_1 \xi^2 + \eta_2 \xi^4}$$

seçilmesi halinde yüksek mertebe Boussinesq denklemine indirgenmektedir.

Eğer $\eta_2 = 0$ seçilirse yüksek mertebeden Boussinesq denklemi,

$$u_{tt} = u_{xx} + \eta_1 u_{xxtt} + (f(u))_{xx}$$

şeklinde literatürde çok iyi bilinen düzgünleştirilmiş (improved) Boussinesq denklemine indirgenir. Son y genelleştirilmiş irmi yılda, genelleştirilmiş düzgünleştirilmiş Boussinesq denklemi hem analitik hem de sayısal bir çok çalışmaya konu olmuştur. Literatürdeki sayısal çalışmalar incelendiği zaman genelleştirilmiş düzgünleştirilmiş Boussinesq denklemini çözmek için sonlu farklar, sonlu elemanlar ve spektral yöntemlerin kullanıldığı gözlenmiştir. Yüksek mertebeden Boussinesq denklemi için sadece analitik çalışmalar yapılmıştır. Duruk ve diğerleri tarafından yüksek mertebe Boussinesq denklemi için tanımlanan Cauchy probleminin $s > \frac{1}{2}$ iken H^s Sobolev uzayında lokal ve global iyi tanımlılığı için gerekli koşullar verilmiştir. Yüksek mertebeden dispersif terimlerin ve doğrusal olmayan farklı kuvvet tipindeki terimlerin sayısal çözümü nasıl etkilediği üzerinde çalışılması gereken konulardan biridir.

Bu tezin amacı yüksek mertebe Boussinesq denklemi için yalnız (soliter) dalga çözümlerini türetmek, denklem için bir sayısal şema önermek, sayısal deneyler yapmak ve şemanın yakınsaklık analizini gerçekleştirmektir.

Tez çalışmasının içeriği aşağıda sunulan şekildedir:

Bölüm 1'de bu tez çalışmasında kullanılacak temel bilgiler sunulmuştur. Bu bağlamda ilk olarak, bazı temel doğrusal cebir kavramları hatırlatılmış, ayrıca önerilen sayısal yöntemin yakınsaklık analizinde kullanılan özel fonksiyon uzayları ve zayıf türev tanımı verilmiştir. Sürekli ve ayrık Fourier açılımları ve Fourier uzayında türev hesabı da yine bu bölümde anlatılmış ve bunlar arasındaki ilişkinin gözlemlenmesi amacıyla üç örnek sunulmuştur. İlk örnekte sıçrama süreksizliğine sahip bir fonksiyon ele alınmış ve bu fonksiyona sürekli ve ayrık Fourier açılımları yardımıyla yaklaşılmaya çalışılmıştır. İkinci örnekte aynı ilişki sürekli bir fonksiyon üzerinde gösterilmiştir. Üçüncü örnekte ise Fourier uzayında türev hesabı gösterilmiştir.

Bölüm 2'de ilk olarak yüksek mertebe Boussinesq denklemi ve literatürde var olan çalışmalar kısaca tanıtılmıştır. HBq denkleminin kütle, enerji ve momentum korunumuna karşı gelen korunan büyüklükleri literatürde türetilmiş olup bu bölümde bu büyüklükler sunulmuştur. Diferansiyel denklemlerin sayısal yöntemlerle çözülmesi durumunda eğer gerçek çözüm bilinmiyorsa hata hesabı yapılamamaktadır. Bu sebeple korunan büyüklüklerin zamanla değişimi sayısal şemanın doğruluğunu test etmek için önemli olmaktadır. Bu nedenle sayısal deneyler kısmında Fourier sözde-spektral (pseudo-spectral) şemanın doğruluğunu test etmek için kütle korunumundan faydalanılacaktır. HBq denklemin yalnız dalga çözümleri de yine bu bölümde türetilmiştir. Bunun için yalnız dalga çözümlerini elde etmede oldukça etkili bir yöntem olan yerine koyma (ansatz) yöntemi kullanılmıştır.

Bölüm 3'te HBq denkleminin sayısal çözümü incelenmiştir. Bunun için bir Fourier sözde-spektral şema önerilmiştir. İlk olarak, sadece uzay değişkeninin ayrıklaştırılması ile elde edilen yarı-ayrık şema ele alınmış ve yarı-ayrık şemanın uygun uzaylarda tanımlanmış başlangıç koşulları altında yakınsaklığı gösterilmiştir. Daha sonra zaman değişkeninin de ayrıklaştırılmasıyla elde edilen tam-ayrık şema sunulmuştur. HBq denkleminin sayısal çözümleri bu tam-ayrık şema yardımıyla hesaplanmıştır. Çözüm adımları şu şekildedir: i) uzay değişkeni için grid noktalarını oluşturulması, ii) denklemin Fourier uzayına taşınması ve burada Fourier katsayıları cinsinden bir adi türevli diferansiyel denklem elde edilmesi, iii) elde edilen denklemin 4. mertebeden Runge-Kutta yöntemi kullanılarak çözülmesi, iv) ters Fourier dönüşümü yardımıyla sayısal çözümün bulunması. Önerilen şema üç faklı problemin çözülmesi için kullanılmıştır: yalnız dalganın yayılımı problemi, iki yalnız dalganın çarpışması problemi ve sonlu zamanda patlayan çözümler. İlk problem olan tek yalnız dalganın yayılımı durumunda HBq denkleminin analitik çözümleri Bölüm 2'de hesaplanmış olduğundan bu problemde gerçek çözüm ile sayısal çözüm arasındaki hata hesaplanabilmiştir. Bu çalışmada farklı kuvvet tipinde doğrusal olmayan terimler göz önüne alınmıştır. Buradan elde ettiğimiz sonuçlar, sunulan sayısal şemanın çok etkili olduğunu göstermektedir. Ayrıca yine bu problemde, kullanılan sayısal şemanın uzayda eksponansiyel yakınsaklığa, zamanda ise 4. mertebe yakınsaklığa sahip olduğu gözlemlenmiştir. Bu sonuçlar beklentilerle uyumludur. Ele alınan diğer problem iki yalnız dalganın çarpışması problemidir. Genel olarak, doğrusal olmayan dalga denklemlerinde verilen parametre değerlerine karşılık farklı hızlarda yayılan yalnız dalgalar elde edilebiliyorken, HBq denklemi için verilen η_1 ve η_2 parametre değerleri için tek bir yalnız dalga çözümü elde edilmektedir. Bu sebeple iki yalnız dalganın çarpışması probleminde eşit hız ve genlikte olan dalgaların çarpışması problemi göz önüne alınmış ve iki örnek sunulmuştur. Burada çarpışmanın elastik olmadığı,

çarpışmadan sonra ortamda çok küçük genlikli ikincil dalgaların varlığı gözlenmiş ve çarpışan dalgaların genlikleri büyüdükçe çarpışmadan sonra oluşan ikincil dalgaların daha belirgin hale geldiği görülmüştür. HBq denklemi ters saçılım yöntemiyle integre edilebilir bir denklem olmadığından bu durum beklentilerimizle uyumludur. Ayrıca iki yalnız dalganın çarpışması probleminde gerçek çözüm elde edilemediğinden sunulan sayısal şemanın doğruluğunu test etmek için kütle korunan büyüklüğünün zamanla değişimi sunulmuştur. Son sayısal örnekte ise sonlu zamanda patlayan çözümler incelenmiştir. Bunun için literatürde analitik olarak verilmiş olan patlama koşullarını sağlayacak başlangıç koşulları seçilmiş ve sayısal çözümün L_∞ normunun zamanla değişimi sunulmuştur.

Bildiğimiz kadarıyla Boussinesq tipi denklemlerle ilgili birçok sayısal çalışma olmasına rağmen literatürde yüksek mertebeden Boussinesq denklemi ile ilgili herhangi bir sayısal çalışmaya rastlanmamıştır. Bu sebeple bu tez çalışmasında sunulan sayısal sonuçlar için bir karşılaştırma yapılamamıştır.

1. THE FOURIER SYSTEM

1.1 Introduction

Fourier series are widely used for many applications in science, engineering and mathematics, such as aircraft and spacecraft guidance, digital signal processing, oil and gas exploration and solution of differential equations. In this chapter some properties of Fourier system, continuous and discrete Fourier expansions will be given. We first recall some basic definitions that will be used in this thesis study. We then review some properties of continuous and discrete Fourier expansions given in [1].

1.2 Preliminaries

Norm: Let V be a complex vector space. A norm is a function $\| \, . \, \| : V \to \mathbb{R}^+$ such that satisfies the following three conditions

1. $\| \, v \, \| \geq 0; \quad \| \, v \, \| = 0 \Leftrightarrow v = 0,$

2. $\| \, cv \, \| = |c| \, \| \, v \, \|,$

3. $\| \, u + v \, \| \;\leq\; \|u\| + \|v\|$ (Triangle Inequality)

for all $u, v \in V$ and $c \in \mathbb{C}$.

Normed Vector Space: A vector space equipped with a norm is called a normed vector space.

Cauchy Sequence: Let V be a normed vector space. A sequence $\{u_k\}_{k=1}^{\infty}$ is called a Cauchy sequence if for any given $\varepsilon > 0$ there is $N > 0$ such that for $n, m \geq N$

$$\| \, u_n - u_m \, \| < \varepsilon.$$

Banach Space: A normed vector space V is said to be complete if every Cauchy sequence is convergent. A complete normed vector space is called as a Banach space.

Inner Product: Let V be a complex vector space. An inner product is a function $(.,.) : V \times V \to \mathbb{C}$ that satisfies the following four conditions

1. $(u,u) \geq 0$; $(u,u) = 0 \Leftrightarrow u = 0$,

2. $(u,v) = \overline{(v,u)}$,

3. $(\alpha u, v) = \overline{\alpha}(u,v)$,

4. $(u+v,w) = (u,w) + (v,w)$

for all $u,v,w \in V$ and $\alpha \in \mathbb{C}$.

Inner Product Space: A complex vector space V with an inner product is called an inner product space. The norm of any vector u in V is defined as

$$\| u \| = \sqrt{(u,u)}.$$

Hilbert Space: If every Cauchy sequence in an inner product space V is convergent, then the vector space V is called as a Hilbert space.

Cauchy-Schwarz Inequality: Let V be an inner product space. If u and $v \in V$ then,

$$|(u,v)| \leq \| u \| \| v \| .$$

Orthogonal Vectors: Let V be an inner product space. Any vectors u and $v \in V$ are orthogonal if $(u,v) = 0$.

Orthogonal Set: Let V be an inner product space. A nonempty set $S \subset V$ is called an orthogonal set if all vectors in S are mutually orthogonal.

Orthonormal Set: An orthogonal set S is called orthonormal if each vector in S is of unit length.

$\mathbf{L^p}(\Omega)$ Space: Let $L^p(\Omega)$ denote the set of p-times Lebesque integrable functions $u : \Omega \to \mathbb{C}$. The $L^p(\Omega)$ norm of $u \in L^p(\Omega)$ is defined by

$$\|u\|_{L^p(\Omega)} = (\int_\Omega |u|^p dx)^{\frac{1}{p}} < \infty, \qquad 1 < p < \infty.$$

$\mathbf{L^\infty}(\Omega)$ Space: Let $L^\infty(\Omega)$ be the space of essentially bounded measurable functions $u : \Omega \to \mathbb{C}$ with norm

$$\|u\|_\infty = \text{ess sup } | u | .$$

Test Function [2]: Let $C_c^\infty(\Omega)$ denote the space of infinitely differentiable functions $\varphi : \Omega \subset (R^n) \to \mathbb{C}$, with compact support in Ω, an open subset of R^n. A function f belonging to $C_c^\infty(\Omega)$ is called a test function.

Compactly Contained Set [2]: Let Ω and V denote open subsets of R^n. We write

$$V \subset\subset \Omega$$

and say V is compactly contained in Ω if $V \subset K \subset \Omega$ for some compact set K.

Locally Integrable Functions [2]: Let $1 \leq p \leq \infty$. $L^p_{loc}(\Omega)$ is the set of locally integrable functions, $L^p_{loc}(\Omega) = \{u : \Omega \to C | u \in L^p(V) \quad \text{for each} \quad V \subset\subset \Omega\}$, i.e $u \in L^p_{loc}(\Omega)$ if $u : \Omega \to C$ satisfies $u \in L^p(V)$ for all $V \subset\subset \Omega$.

Weak Derivative [2]: Suppose $u, v \in L^1_{loc}(U)$ and α is multiindex. If the equality

$$\int_U u D^\alpha \phi dx = (-1)^{|\alpha|} \int_U v \phi dx$$

is satisfied for all test functions $\phi \in C_c^\infty$, then v is called the weak derivative of order $| \alpha |$ of the function u in the domain U and is denoted by $D^\alpha u$ i.e. $v = D^\alpha u$.

Sobolev Space [2]: The Sobolev space $W^{k,p}(U)$ consists of all integrable functions $u : U \to R$ such that for each multiindex α with $| \alpha | \leq k$, $D^\alpha u$ exists in the weak sense and belongs to $L^p(U)$. Similarly we define the space $W^{k,p}_{loc}(U)$ using locally integrable functions instead of integrable ones. We introduce a natural norm on the Sobolev space:

$$\| u \|_{W^{k,p}} = \sum_{|\alpha| \leq k} \| D^\alpha u \|_{L^p} .$$

1.3 Continuous Fourier Expansion

We use $(.,.)$ and $\|.\|$ to denote the inner product and the norm of $L^2(\Omega)$ defined by

$$(u, v) = \int_{-L}^{L} u(x)\overline{v(x)}dx, \quad \|u\| = \sqrt{(u, u)} \tag{1.1}$$

for $\Omega = (-L, L)$, respectively. The set of functions $\phi_k(x) = e^{ik\pi x/L}$, $k \in \mathbb{Z}$ construct an orthogonal system over the interval $(-L, L)$:

$$\int_{-L}^{L} \phi_k(x)\overline{\phi_l(x)}dx = 2L\delta_{kl} = \begin{cases} 0 & \text{if } k \neq l \\ 2L & \text{if } k = l. \end{cases} \tag{1.2}$$

Let u be a piecewise smooth function on $[-L, L]$. The Fourier series of the function u can be written as

$$u(x) = \sum_{k=-\infty}^{\infty} \widehat{u}_k e^{ik\pi x/L}$$

where

$$\widehat{u}_k = \frac{1}{2L}\int_{-L}^{L} u(x)e^{-ik\pi x/L}dx\ , \quad k \in \mathbb{Z} \tag{1.3}$$

are called Fourier coefficients of u. The Fourier series converges to $u(x)$ at all points where u is continuous, and to $\frac{u(x+)+u(x-)}{2}$ at all points where u is discontinuous. $\frac{u(x+)+u(x-)}{2}$ is the mean value of the right- and left-hand limits at the point x.

Let S_N be the space of trigonometric polynomials of degree up to $N/2$ defined as:

$$S_N = span\{e^{ik\pi x/L}|\ \ -N/2 \le k \le N/2-1\}.$$

where N is a positive even integer. $P_N : L^2(\Omega) \to S_N$ is the orthogonal projection operator given by

$$P_N u(x) = \sum_{k=-N/2}^{N/2-1} \widehat{u}_k e^{ik\pi x/L}.$$

Then by using the orthogonality relation we have

$$(u,\varphi) = (P_N u,\varphi) \ \text{ for } \ \text{all } \ \varphi \ \in \ S_N. \tag{1.4}$$

To measure how well the N^{th} partial sum $P_N u$ approximate to u, the mean square error defined by

$$E_N(u) = \frac{1}{2L}\int_{-L}^{L} |u(x) - P_N u(x)|^2 dx. \tag{1.5}$$

Note that $|u - P_N u|$ denotes the complex modulus. Expanding the right hand side of the equation (1.5), we have

$$\begin{aligned} E_N(u) &= \frac{1}{2L}\int_{-L}^{L} (u(x) - P_N u(x))\overline{(u(x) - P_N u(x))}dx \\ &= \frac{1}{2L}\int_{-L}^{L} |u(x)|^2 + |P_N u(x)|^2 - 2Re\{u(x)\overline{P_N u(x)}\}dx. \end{aligned} \tag{1.6}$$

Note that

$$\begin{aligned} \frac{1}{2L}\int_{-L}^{L} |P_N u(x)|^2 dx &= \frac{1}{2L}\int_{-L}^{L} P_N u(x)\overline{P_N u(x)}dx \\ &= \frac{1}{2L}\int_{-L}^{L} \sum_{k=-N/2}^{N/2-1} \widehat{u}_k e^{ik\pi x/L} \overline{\sum_{l=-N/2}^{N/2-1} \widehat{u}_l e^{il\pi x/L}}dx \\ &= \frac{1}{2L}\int_{-L}^{L} \sum_{k=-N/2}^{N/2-1}\sum_{l=-N/2}^{N/2-1} \widehat{u}_k\overline{\widehat{u}_l} e^{ik\pi x/L}e^{-il\pi x/L}dx \\ &= \frac{1}{2L}\sum_{k=-N/2}^{N/2-1}\sum_{l=-N/2}^{N/2-1} \widehat{u}_k\overline{\widehat{u}_l}\int_{-L}^{L} e^{ik\pi x/L}e^{-il\pi x/L}dx \\ &= \sum_{k=-N/2}^{N/2-1} |\overline{\widehat{u}_k}|^2 \end{aligned}$$

where we have taken advantage of orthogonal system (1.2). On the other hand,

$$\begin{aligned}
\frac{1}{2L}\int_{-L}^{L} u(x)|P_N u(x)|dx &= \frac{1}{2L}\int_{-L}^{L} u(x)\sum_{k=-N/2}^{N/2-1}\overline{\widehat{u}_k e^{ik\pi x/L}}dx \\
&= \frac{1}{2L}\int_{-L}^{L}\sum_{k=-N/2}^{N/2-1}\overline{\widehat{u}_k}u(x)e^{-ik\pi x/L}dx \\
&= \sum_{k=-N/2}^{N/2-1}\frac{\overline{\widehat{u}_k}}{2L}\int_{-L}^{L} u(x)e^{-ik\pi x/L}dx \\
&= \sum_{k=-N/2}^{N/2-1}|\widehat{u}_k|^2.
\end{aligned}$$

Theorem 1: Let $u \in L^2[-L,L]$ with complex Fourier coefficients $\widehat{u}_k$ given by (1.3). Then

$$E_N(u) = \frac{1}{2L}\int_{-L}^{L}|u(x)|^2dx - \sum_{k=-N/2}^{N/2-1}|\widehat{u}_k|^2.$$

It can be shown that

$$\lim_{N\to\infty} E_N(u) = 0$$

for any square integrable function on $[-L,L]$, from which it follows the following statement.

Parseval Identity: If $u \in L^2(-L,L)$, then its Fourier series converges to u ,

$$\frac{1}{2L}\int_{-L}^{L}|u(x)|^2dx = \sum_{k=-\infty}^{\infty}|\widehat{u}_k|^2.$$

Now the question arises as to what the rate of convergence for the Fourier series is. For convenience, we set

$$\sum_{|k|\gtrsim N/2} \equiv \sum_{\substack{k<-N/2 \\ k\geq N/2}}.$$

From the Parseval identity one has

$$\| u - P_N u \| = (2L\sum_{|k|\gtrsim N/2}|\widehat{u}_k|^2)^{1/2}.$$

If u is sufficiently smooth,

$$\max_{-L\leq x\leq L} | u(x) - P_N u(x) | \leq \sum_{|k|\gtrsim N/2}|\widehat{u}_k|$$

This inequality shows that the size of the error created by replacing u with $P_N u$ depends upon how fast the Fourier coefficients of u decay to zero. For continuously differentiable u

$$2L\widehat{u}_k = \int_{-L}^{L} u(x)e^{-ik\pi x/L}dx = -\frac{1}{ik}(u(L-)-u(-L+)) + \frac{1}{ik}\int_{-L}^{L} u'(x)e^{-ik\pi x/L}dx.$$

Thus, we observe the behaviour of the Fourier coefficient $\widehat{u}_k$ as k^{-1} so

$$\widehat{u}_k = O(k^{-1}).$$

Let u be m times continuously differentiable in $[-L,L]$ $(m \geq 1)$ and $u^{(j)}$ be periodic for all $j \leq m-2$. If we iterate the above argument, then we have

$$\widehat{u}_k = O(k^{-m}), \quad k = \pm 1, \pm 2, \pm 3 \ldots .$$

The k^{th} Fourier coefficient of a function decays faster than its negative powers which is an indication of spectral or exponential accuracy.

1.4 Discrete Fourier Expansion

For $N > 0$, consider the set of points (nodes or grid points)

$$x_j = -L + \frac{2L}{N} j, \quad j = 0, 1, \ldots N-1 .$$

Let also consider to know $u(x_j)$ the value of complex function u at the grid point x_j. The discrete Fourier coefficients are given by

$$\widetilde{u}_k = \mathscr{F}_k[u(x_j)] = \frac{1}{N}\sum_{j=0}^{N-1} u(x_j)e^{-ik\pi x_j/L}, \quad k = -N/2, \ldots, N/2-1.$$

Conversely, by using orthogonality the inversion formula gives

$$u(x_j) = \mathscr{F}_j^{-1}[\widetilde{u}_k] = \sum_{k=-N/2}^{N/2-1} \widetilde{u}_k e^{ik\pi x_j/L}, \quad j = 0, 1, 2, \ldots, N-1.$$

Hence,

$$I_N u(x) = \sum_{k=-N/2}^{N/2-1} \widetilde{u}_k e^{ik\pi x/L}$$

is the $\frac{N}{2}-$degree trigonometric interpolation of u at the grid points and satisfies

$$I_N u(x_j) = u(x_j), \quad j = 0, 1, \ldots N-1 .$$

which is known as the discrete Fourier series of u. The discrete Fourier coefficients $\widetilde{u}_k, \quad k = N/2, ...N/2-1$ depend on the values of u at the grid points. The discrete Fourier transform (DFT) is the mapping between $u(x_j)$ and $\widetilde{u}_k$. If the Fourier series of a function u converges to itself at every point then discrete Fourier coefficients can be written in terms of continuous Fourier coefficients as

$$\widetilde{u}_k = \widehat{u}_k + \sum_{\substack{m=-\infty \\ m\neq 0}}^{\infty} \widehat{u}_{k+Nm}, \quad k = -N/2, ..., N/2-1$$

An equivalent formulation is

$$I_N u(x) = P_N u(x) + R_N u(x),$$

with

$$R_N u(x) = \sum_{k=-N/2}^{N/2-1} (\sum_{\substack{m=-\infty \\ m\neq 0}}^{\infty} \widehat{u}_{k+Nm}) \phi_k.$$

$R_N u(x)$ is called the aliasing error and it is orthogonal to the truncation error [1], $u - P_N u$, so that

$$\|u - I_N u\|^2 = \|u - P_N u\|^2 + \|R_N u(x)\|^2.$$

This shows that the error due to the interpolation is always larger than the error due to truncation. The influence of the aliasing on the accuracy of the spectral methods is asymptotically of the same order as the truncation error [1].

Example 1: Consider the function

$$u(x) = \begin{cases} 1 \quad \text{if} \quad -\pi/2 < x \leq \pi/2 \\ \\ 0 \quad \text{if} \quad -\pi \leq x \leq -\pi/2, \ \pi/2 < x \leq \pi. \end{cases}$$

Its continous Fourier coefficients are computed as

$$\hat{u}_k = \begin{cases} \frac{1}{2} & \text{if } k = 0 \\ \\ 0 & \text{if } k \neq 0 \text{ , } k \text{ even} \\ \\ \frac{1}{\pi} \frac{(-1)^{\frac{k-1}{2}}}{k} & \text{if } k \neq 0 \text{ , } k \text{ odd} \end{cases}$$

In Figure 1.1 and 1.2, we compare trigonometric approximations $P_N u$ and $I_N u$ with the exact function $u(x)$ for $N = 16,\ 32$, respectively.

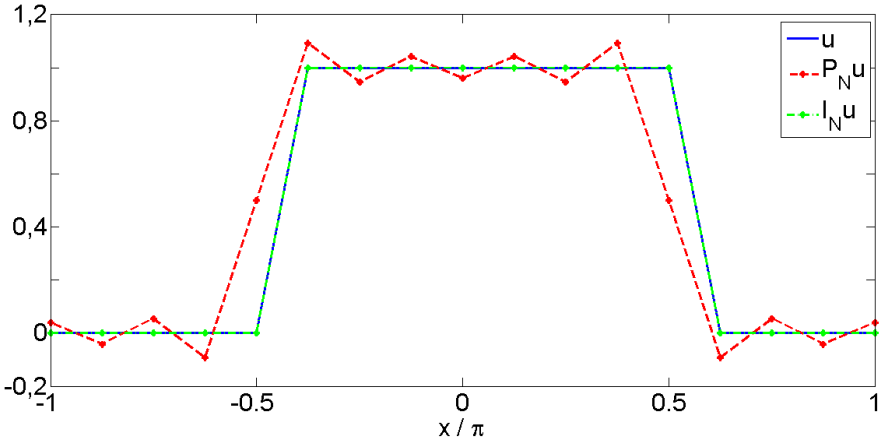

Figure 1.1: Comparison $P_N u$, $I_N u$ and exact solution $u(x)$ for $N = 16$

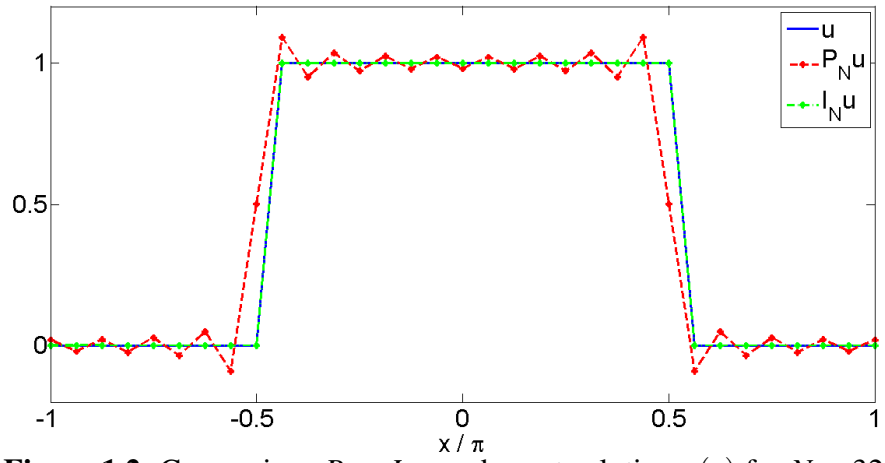

Figure 1.2: Comparison $P_N u$, $I_N u$ and exact solution $u(x)$ for $N = 32$

Example 2: Consider the function

$$u(x) = \cos(\frac{x}{2})$$

is infinitely differentiable in $[-\pi, \pi]$, but $u'(-\pi+) \neq u'(\pi-)$. Its Fourier coefficients are

$$\widehat{u}_k = \frac{2}{\pi} \frac{(-1)^k}{1-4k^2}.$$

In Figure 1.3, 1.4 and 1.5 we again compare trigonometric approximations $P_N u$ and $I_N u$ with the exact function $u(x)$ for $N = 8,\ 16,\ 32$, respectively. For this example we say the convergence of the truncated series is quadratic except at the end points since the coefficients $\widehat{u}_k$ decay quadratically.

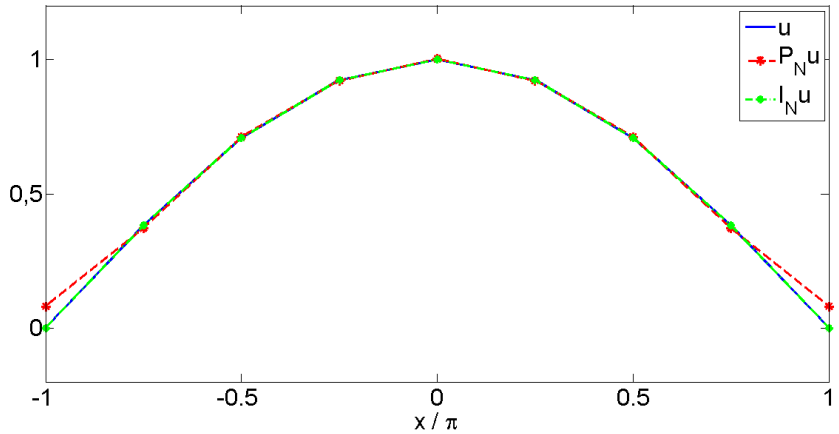

Figure 1.3: Comparison $P_N u$, $I_N u$ and exact solution $u(x)$ for $N = 8$

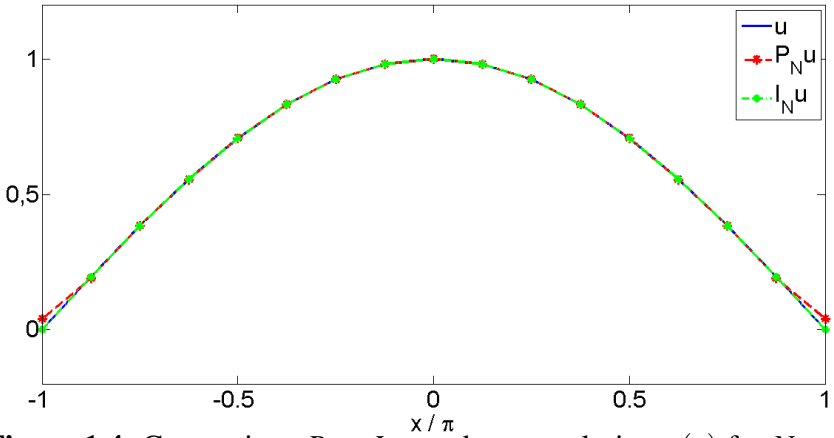

Figure 1.4: Comparison $P_N u$, $I_N u$ and exact solution $u(x)$ for $N = 16$

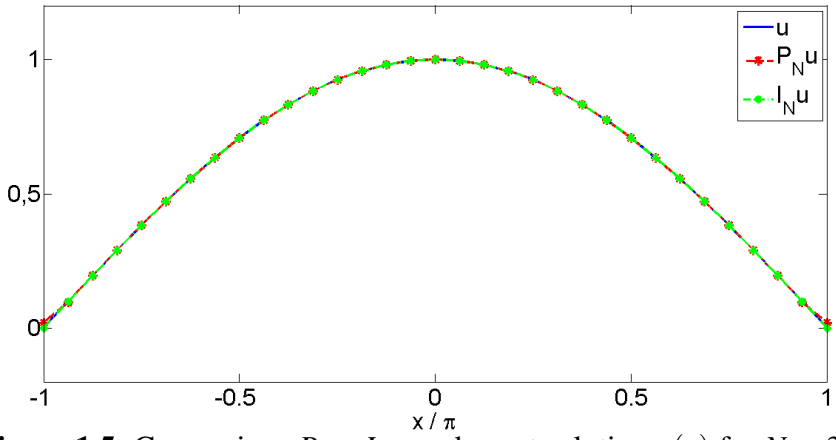

Figure 1.5: Comparison $P_N u$, $I_N u$ and exact solution $u(x)$ for $N = 32$

1.5 Differentiation in Spectral Methods

If the Fourier series of u is given by

$$u = \sum_{k=-\infty}^{\infty} \widehat{u}_k \phi_k,$$

then the Fourier series of u' is

$$u' = \sum_{k=-\infty}^{\infty} \frac{ik\pi}{L} \widehat{u}_k \phi_k.$$

Therefore,

$$(P_N u)' = P_N u'$$

i.e. truncation and differentiation commute. Now the question arises whether the interpolation and differentiation operators commute or not. The approximate derivative at the grid points are given by

$$(I_N u)'(x_j) = \sum_{k=-N/2}^{N/2-1} a_k e^{ik\pi x_j/L}$$

where

$$a_k = \frac{ik\pi}{L} \widetilde{u}_k, \quad k = -N/2, \ldots, N/2-1 \ .$$

The function $(I_N u)'$ is called the Fourier collocation derivative of u. From discussion above we generally get

$$(I_N u)' \neq P_N u'. \tag{1.7}$$

The function $I_N u'$ is called the Fourier interpolation derivative of u. Interpolation and differentiation do not commute, i.e

$$(I_N u)' \neq I_N(u') \quad \text{unless} \quad u \in S_N. \tag{1.8}$$

It has been proved in [3] that the error $(I_N u)' - I_N(u')$ is the same order as the truncation error for the derivative $u' - P_N(u')$. This shows that interpolation differentiation is spectrally accurate. In order to see the relation (1.7) and (1.8) we consider following example.

Example 3: Consider the function

$$u(x) = \cos(\frac{x}{2}).$$

This function is infinitely differentiable in $[-\pi, \pi]$, but $u'(-\pi+) \neq u'(\pi-)$. In Figure 1.6, 1.7 and 1.8, $P_N u'$, $(I_N u)'$, $I_N u'$ and $u'(x)$ are compared for $N = 8$, 16, 32, respectively.

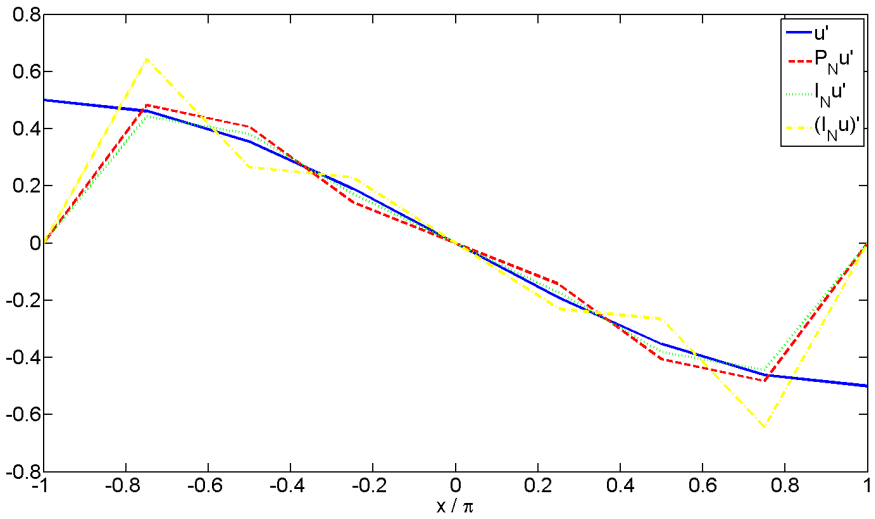

Figure 1.6: $P_N u'$, $(I_N u)'$, $I_N u'$ and $u'(x)$ for $N = 8$

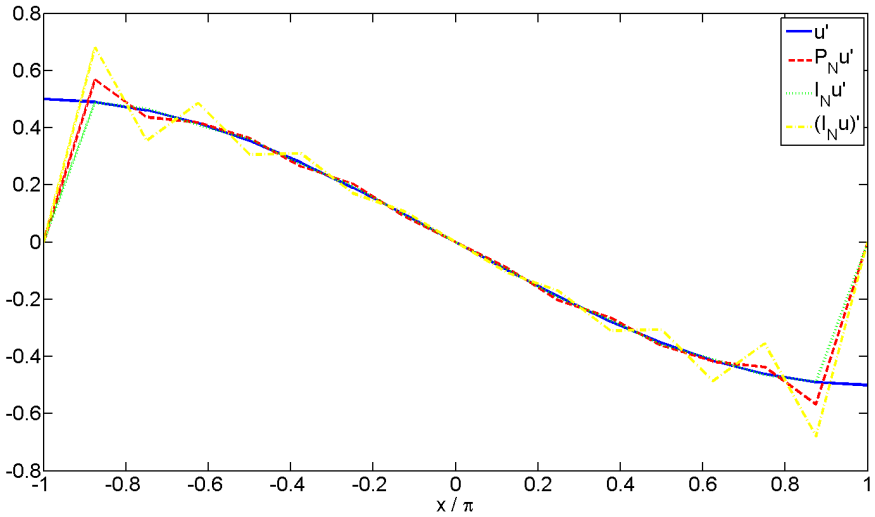

Figure 1.7: $P_N u'$, $(I_N u)'$, $I_N u'$ and $u'(x)$ for $N = 16$

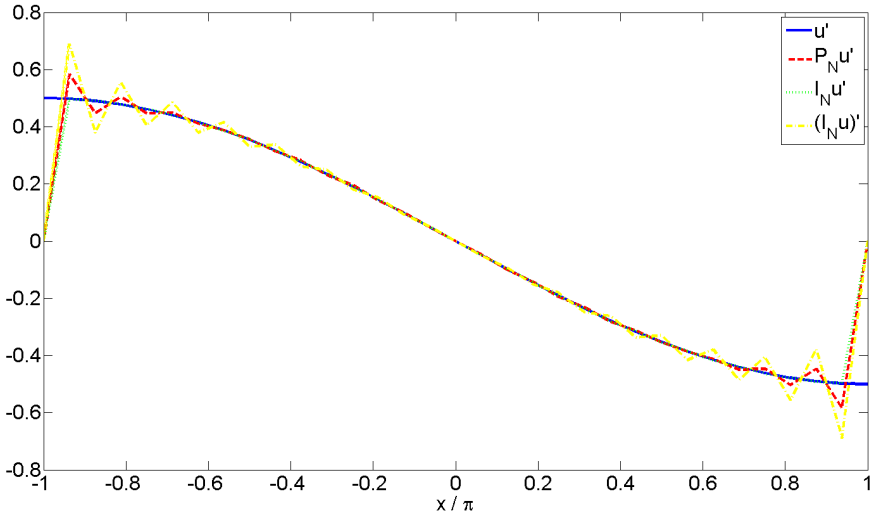

Figure 1.8: $P_N u'$, $(I_N u)'$, $I_N u'$ and $u'(x)$ for $N = 32$

2. THE HIGHER-ORDER BOUSSINESQ EQUATION

2.1 Introduction

In this chapter, we introduce the higher-order Boussinesq equation. In Section 2.2, we present some brief information about the literature and the conserved quantities. In Section 2.3 we use the ansatz method to derive the solitary wave solutions of the higher-order Boussinesq equation.

2.2 The Higher-Order Boussinesq Equation

In this thesis study, we consider the higher order Boussinesq (HBq) equation with the following initial conditions

$$u_{tt} = u_{xx} + \eta_1 u_{xxtt} - \eta_2 u_{xxxxtt} + (f(u))_{xx} \tag{2.1}$$

$$u(x,0) = \phi(x), \qquad u_t(x,0) = \psi(x). \tag{2.2}$$

where $f(u) = u^p$ and $p > 1$ is integer. Here η_1 and η_2 are real positive constants. The independent variables x and t denote spatial coordinate and time, respectively. The HBq equation was first derived by Rosenau [4] for the continuum limit of a dense chain of particles with elastic couplings. The same equation was used to model water waves with surface tension by Schneider & Wayne [5]. The HBq equation has also been derived to model the propagation of longitudinal waves in an infinite elastic medium with nonlinear and nonlocal properties by Duruk et al in [6]. Three conserved quantities for the HBq equation are derived in [4, 7] in terms of U where $u = U_x$. The conserved quantities corresponding to mass, momentum and energy are respectively:

$$\mathscr{M}(t) = \int_{-\infty}^{\infty} U_t \, dx, \tag{2.3}$$

$$\mathscr{P}(t) = \int_{-\infty}^{\infty} U_x [U_t - \eta_1 U_{xxt} + \eta_2 U_{xxxxt}] \, dx \tag{2.4}$$

$$\mathscr{E}(t) = \int_{-\infty}^{\infty} (U_t)^2 + 2F(U_x) + \eta_1 (U_{xt})^2 + \eta_2 (U_{xxt})^2 \, dx \tag{2.5}$$

where $f(s) = F'(s)$.

2.3 Solitary Wave Solution

We will use the ansatz method which is the most effective direct method to construct the solitary wave solutions of the nonlinear evolution equations. We look for the solutions of the form $u = u(\xi)$ where $\xi = x - ct - x_0$. Assume that u and all their derivatives converge to zero sufficiently rapidly as $\xi \to \pm\infty$. Substituting the solution $u = u(\xi)$ into eq. (2.1) yields a sixth order ordinary differential equation

$$(c^2 - 1)u'' - \eta_1 c^2 \frac{d^4u}{d\xi^4} + \eta_2 c^2 \frac{d^6u}{d\xi^6} = (u^p)'' \tag{2.6}$$

and then integrating twice with respect to ξ, we have

$$(c^2 - 1)u - \eta_1 c^2 \frac{d^2u}{d\xi^2} + \eta_2 c^2 \frac{d^4u}{d\xi^4} = u^p + c_1\xi + c_2 \tag{2.7}$$

where c_1 and c_2 are arbitrary integration constants. Setting $c_1 = c_2 = 0$ from the boundary conditions, the equation (2.7) becomes

$$(c^2 - 1)u - \eta_1 c^2 \frac{d^2u}{d\xi^2} + \eta_2 c^2 \frac{d^4u}{d\xi^4} = u^p. \tag{2.8}$$

We now look for the solution of the form

$$u(\xi) = A\mathrm{sech}^{\gamma}(B\xi). \tag{2.9}$$

To use the above ansatz on the equation (2.7) we need the following derivatives

$$\begin{aligned}
u'(\xi) &= AB\gamma\mathrm{sech}^{\gamma}(B\xi)\tanh(B\xi),\\
u''(\xi) &= AB^2\gamma\mathrm{sech}^{\gamma}(B\xi)[\gamma - (\gamma+1)\mathrm{sech}^2(B\xi)],\\
u^{(IV)}(\xi) &= AB^4\gamma\mathrm{sech}^{\gamma}(B\xi)[\gamma^3 - 2(2+4\gamma+3\gamma^2+\gamma^3)\mathrm{sech}^2(B\xi)\\
&\qquad +(6+11\gamma+6\gamma^2+\gamma^3)\mathrm{sech}^4(B\xi)].
\end{aligned}$$

Substituting these derivatives into the equation (2.8),

$$\begin{aligned}
(c^2-1)A\mathrm{sech}^{\gamma}(B\xi) &- \eta_1 c^2 AB^2\gamma\mathrm{sech}^{\gamma}(B\xi)[\gamma - (\gamma+1)\mathrm{sech}^2(B\xi)]\\
&+\eta_2 c^2 AB^4\gamma\mathrm{sech}^{\gamma}(B\xi)[\gamma^3 - 2(2+4\gamma+3\gamma^2+\gamma^3)\mathrm{sech}^2(B\xi)\\
&+(6+11\gamma+6\gamma^2+\gamma^3)\mathrm{sech}^4(B\xi)] - A^p\mathrm{sech}^{\gamma p}(B\xi) = 0.
\end{aligned} \tag{2.10}$$

Equating the exponents $\gamma+4$ and γp in (2.10), we have

$$\gamma = \frac{4}{p-1}\,.$$

Note that $\text{sech}^{\gamma+4}(B\xi)$, $\text{sech}^{\gamma+2}(B\xi)$ and $\text{sech}^{\gamma}(B\xi)$ are linearly independent functions. By setting their respective coefficients in (2.10) to zero, we obtain the following equations:

$$\eta_2 c^2 A B^4 \gamma(\gamma^3+6\gamma^2+11\gamma+6) = A^p \tag{2.11}$$

$$\eta_1 c^2 A B^2 \gamma(\gamma+1) - 2\eta_2 c^2 A B^4 \gamma(\gamma^3+3\gamma^2+4\gamma+2) = 0 \tag{2.12}$$

$$(c^2-1)A - \eta_1 c^2 A B^2 \gamma^2 + \eta_2 c^2 A B^4 \gamma^4 = 0. \tag{2.13}$$

Finally, the HBq equation admits the solitary wave solution as

$$u(x,t) = A\left\{\text{sech}^4\left(B(x-ct-x_0)\right)\right\}^{\frac{1}{p-1}},$$

$$A = \left[\frac{\eta_1^2 c^2 (p+1)\,(p+3)\,(3p+1)}{2\eta_2\,(p^2+2p+5)^2}\right]^{\frac{1}{p-1}}, \quad B = \left[\frac{\eta_1 (p-1)^2}{4\eta_2 (p^2+2p+5)}\right]^{\frac{1}{2}},$$

$$c^2 = \left\{1 - \left[\frac{4\eta_1^2\,(p+1)^{\,2}}{\eta_2\,(p^2+2p+5)^2}\right]\right\}^{-1}.$$

where A is amplitude, B is the inverse width of the solitary wave and c represents velocity of the solitary wave at x_0 with $c^2 > 1$.

3. THE PSEUDO-SPECTRAL METHOD FOR THE HIGHER-ORDER BOUSSINESQ EQUATION

3.1 Introduction

In this chapter, we propose a Fourier pseudo-spectral method for solving the higher-order Boussinesq equation with various power type nonlinear terms. In Section 3.2, we prove the convergence of the semi-discrete scheme in the appropriate energy space. In Section 3.3, we propose the fully-discrete scheme for solving the HBq equation. In Section 3.4, we present some numerical experiments to verify the accuracy of the proposed scheme.

3.2 The Semi-Discrete Scheme

Let $H_p^s(\Omega)$ denote the periodic Sobolev space equipped with the norm

$$\|u\|_s^2 = \sum_{k=-\infty}^{\infty} (1+|k|^{2s})|\hat{u}_k|^2$$

where $\hat{u}_k = \dfrac{1}{2L}\displaystyle\int_\Omega u(x)e^{-ik\pi x/L}dx$. The Banach space $X_s = C^1([0,T];H_p^s(\Omega))$ is the space of all continuous functions in $H_p^s(\Omega)$ whose distributional derivative is also in $H_p^s(\Omega)$, with the norm $\|u\|_{X_s}^2 = \max\limits_{t\in[0,T]}(\|u(t)\|_s^2 + \|u_t(t)\|_s^2)$. Throughout this section, C denotes a generic constant. In order to obtain the convergence of semi-discrete scheme, we need following lemmas.

Lemma 1 [8,9]: For any real $0 \le \mu \le s$, there exists a constant C such that

$$\|u - P_N u\|_\mu \le CN^{\mu-s}\|u\|_s \qquad \forall u \in H_p^s(\Omega).$$

Lemma 2 [10]: Assume that $f \in C^k(\mathbb{R})$, $u, v \in H^s(\Omega)\cap L^\infty(\Omega)$ and $k = [s]+1$, where $s \ge 0$. Then we have

$$\|f(u) - f(v)\|_s \le C(M)\|u - v\|_s$$

if $\|u\|_\infty \le M, \|v\|_\infty \le M, \|u\|_s \le M$ and $\|v\|_s \le M$, where $C(M)$ is a constant dependent on M and s.

Corollary 1: Assume that $f \in C^3(\mathbb{R})$ and $u, v \in H^2(\Omega) \cap L^\infty(\Omega)$ then

$$\|f(u) - f(v)\|_2 \leq C\|u - v\|_2$$

where C is a constant dependent on $\|u\|_\infty, \|v\|_\infty$ and $\|u\|_2, \|v\|_2$.

Gronwall Lemma: Suppose nonnegative $x(t)$ satisfies the following differential inequality

$$\frac{dx(t)}{dt} \leq g(t)x(t) + h(t)$$

where $g(t)$ is a continuous and $h(t)$ is a locally integrable functions. Then, $x(t)$ satisfies

$$x(t) \leq x(0)e^{G(t)} + \int_0^t e^{G(t)-G(s)}h(s)ds$$

where

$$G(t) = \int_0^t g(r)dr.$$

3.2.1 Convergence of the semi-discrete scheme

The semi-discrete Fourier pseudo-spectral scheme for (2.1)-(2.2) is

$$u^N_{tt} = u^N_{xx} + \eta_1 u^N_{xxtt} - \eta_2 u^N_{xxxxtt} + P_N f(u^N)_{xx}, \tag{3.1}$$

$$u^N(x,0) = P_N\phi(x), \qquad u^N_t(x,0) = P_N\psi(x) \tag{3.2}$$

where $u^N(x,t) \in S_N$ for $0 \leq t \leq T$. We now state our main result.

Theorem 2: Let $s \geq 2$ and $u(x,t)$ be the solution of the periodic initial value problem (2.1)-(2.2) satisfying $u(x,t) \in C^1([0,T];H^s_p(\Omega))$ for any $T > 0$ and $u^N(x,t)$ be the solution of the semi-discrete scheme (3.1)-(3.2). There exists a constant C, independent of N, such that

$$\|u - u^N\|_{X_2} \leq C(T, \eta_1, \eta_2)N^{2-s}\|u\|_{X_s}$$

for the initial data $\phi, \psi \in H^s_p(\Omega)$.

Proof: Using the triangle inequality it is possible to write

$$\|u - u^N\|_{X_2} \leq \|u - P_N u\|_{X_2} + \|P_N u - u^N\|_{X_2}. \tag{3.3}$$

Using Lemma 1, we have the following estimates

$$\|(u - P_N u)(t)\|_2 \leq CN^{2-s}\|u(t)\|_s$$

and

$$\|(u - P_N u)_t(t)\|_2 \leq CN^{2-s}\|u_t(t)\|_s$$

for $s \geq 2$. Taking the maximum values of both sides gives

$$\max_{t\in[0,T]}(\|(u-P_Nu)(t)\|_2+\|(u-P_Nu)_t(t)\|_2) \leq C\,N^{2-s}\max_{t\in[0,T]}(\|u(t)\|_s+\|u_t(t)\|_s).$$

Thus, the estimation of the first term at the right-hand side of the inequality (3.3) becomes

$$\|u-P_Nu\|_{X_2} \leq CN^{2-s}\|u\|_{X_s}. \tag{3.4}$$

Now, we need to estimate the second term $\|P_Nu-u^N\|_{X_2}$ at the right-hand side of the inequality (3.3). Subtracting the equation (3.1) from (2.1) and taking the inner product with $\varphi \in S_N$ we have

$$\big((u-u^N)_{tt}-(u-u^N)_{xx}-\eta_1(u-u^N)_{xxtt}+\eta_2(u-u^N)_{xxxxtt}-(f(u)-P_Nf(u^N))_{xx},\ \varphi\big)=0. \tag{3.5}$$

Since

$$((u-P_Nu)_{tt},\varphi)=((u-P_Nu)_{xx},\varphi)=((u-P_Nu)_{xxtt},\varphi)=((u-P_Nu)_{xxxxtt},\varphi)=0$$

for all $\varphi \in S_N$ and by $D_x^nP_Nu = P_ND_x^nu$ and $D_t^nP_Nu = P_ND_t^nu$ the equation (3.5) becomes

$$\begin{aligned}\big((P_Nu-u^N)_{tt}-(P_Nu-u^N)_{xx}-\eta_1(P_Nu-u^N)_{xxtt}+\eta_2(P_Nu-u^N)_{xxxxtt}\\ -(f(u)-P_Nf(u^N))_{xx},\ \varphi\big)=0\end{aligned} \tag{3.6}$$

for all $\varphi \in S_N$. Setting $\varphi=(P_Nu-u^N)_t$ in (3.6), using the integration by parts and the spatial periodicity, a simple calculation shows that

$$\big((P_Nu-u^N)_{tt},\ (P_Nu-u^N)_t\big)=\frac{1}{2}\frac{d}{dt}\|(P_Nu-u^N)_t(t)\|^2, \tag{3.7}$$

$$\big((P_Nu-u^N)_{xx},\ (P_Nu-u^N)_t\big)=-\frac{1}{2}\frac{d}{dt}\|(P_Nu-u^N)_x(t)\|^2, \tag{3.8}$$

$$\big((P_Nu-u^N)_{xxtt},\ (P_Nu-u^N)_t\big)=-\frac{1}{2}\frac{d}{dt}\|(P_Nu-u^N)_{xt}(t)\|^2, \tag{3.9}$$

$$\big((P_Nu-u^N)_{xxxxtt},\ (P_Nu-u^N)_t\big)=\frac{1}{2}\frac{d}{dt}\|(P_Nu-u^N)_{xxt}(t)\|^2. \tag{3.10}$$

Substituting (3.7) - (3.10) in (3.6), we have

$$\begin{aligned}&\frac{1}{2}\frac{d}{dt}(\|(P_Nu-u^N)_t(t)\|^2+\|(P_Nu-u^N)_x(t)\|^2+\eta_1\|(P_Nu-u^N)_{xt}(t)\|^2\\ &\quad+\eta_2\|(P_Nu-u^N)_{xxt}(t)\|^2)=\big((f(u)-f(u^N))_{xx},(P_Nu-u^N)_t\big).\end{aligned} \tag{3.11}$$

In the following, we will estimate the right-hand side of the above equation. Using the Cauchy-Schwarz inequality and the Corollary 1, we have

$$\begin{aligned}
|((f(u)-f(u^N))_{xx},\ (P_Nu-u^N)_t)| &\leq \|(f(u)-f(u^N))_{xx}\|\ \|(P_Nu-u^N)_t(t)\| \\
&\leq \frac{1}{2}\left(\|f(u)-f(u^N)_{xx}\|^2+\|(P_Nu-u^N)_t(t)\|^2\right) \\
&\leq \frac{1}{2}\left(\|f(u)-f(u^N)\|_2^2+\|(P_Nu-u^N)_t(t)\|^2\right) \\
&\leq C\left(\|(u-u^N)(t)\|_2^2+\|(P_Nu-u^N)_t(t)\|^2\right).
\end{aligned} \tag{3.12}$$

Substituting (3.12) in (3.11) we have

$$\begin{aligned}
\frac{1}{2}\frac{d}{dt}(&\|(P_Nu-u^N)_t(t)\|^2+\|(P_Nu-u^N)_x(t)\|^2+\eta_1\|(P_Nu-u^N)_{xt}(t)\|^2 \\
&\qquad +\eta_2\|(P_Nu-u^N)_{xxt}(t)\|^2) \\
&\leq C\left(\|(u-u^N)(t)\|_2^2+\|(P_Nu-u^N)_t(t)\|^2\right) \\
&\leq C\left(\|(u-P_Nu)(t)\|_2^2+\|(P_Nu-u^N)(t)\|_2^2+\|(P_Nu-u^N)_t(t)\|^2\right).
\end{aligned} \tag{3.13}$$

Adding the terms $\left(P_Nu-u^N,\ (P_Nu-u^N)_t\right)$ and $\left((P_Nu-u^N)_{xx},\ (P_Nu-u^N)_{xxt}\right)$ to both sides, the equation (3.13) becomes

$$\begin{aligned}
\frac{1}{2}\frac{d}{dt}\Big(&\ \|(P_Nu-u^N)_t(t)\|^2+\|(P_Nu-u^N)_x(t)\|^2+\eta_1\|(P_Nu-u^N)_{xt}(t)\|^2 \\
&\quad +\eta_2\|(P_Nu-u^N)_{xxt}(t)\|^2+\|(P_Nu-u^N)(t)\|^2+\|(P_Nu-u^N)_{xx}(t)\|^2\ \Big) \\
&\leq C\Big(\ \|(u-P_Nu)(t)\|_2^2+\|(P_Nu-u^N)(t)\|_2^2+\|(P_Nu-u^N)_t(t)\|^2 \\
&\quad +\frac{1}{2}\|(P_Nu-u^N)(t)\|^2+\frac{1}{2}\|(P_Nu-u^N)_t(t)\|^2 \\
&\quad +\frac{1}{2}\|(P_Nu-u^N)_{xx}(t)\|^2+\frac{1}{2}\|(P_Nu-u^N)_{xxt}(t)\|^2\ \Big) \\
&\leq C\left(\ \|(u-P_Nu)(t)\|_2^2+\|(P_Nu-u^N)(t)\|_2^2+\|(P_Nu-u^N)_t(t)\|_2^2\ \right).
\end{aligned} \tag{3.14}$$

Therefore,

$$\begin{aligned}
\frac{1}{2}\min\{1,\eta_1,\eta_2\}\frac{d}{dt}&\left[\ \|(P_Nu-u^N)(t)\|_2^2+\|(P_Nu-u^N)_t(t)\|_2^2\ \right] \\
&\leq C\left(\ \|(u-P_Nu)(t)\|_2^2+\|(P_Nu-u^N)(t)\|_2^2+\|(P_Nu-u^N)_t(t)\|_2^2\ \right).
\end{aligned}$$

Note that $\|(P_N u - u^N)(0)\|_2 = 0$ and $\|(P_N u - u^N)_t(0)\|_2 = 0$. The Gronwall Lemma and Lemma 1 imply that

$$\begin{aligned}
\|(P_N u - u^N)(t)\|_2^2 + \|(P_N u - u^N)_t(t)\|_2^2 &\leq \int_0^t \|u(\tau) - P_N u(\tau)\|_2^2 \, e^{C_1(t-\tau)} d\tau \\
&\leq C_2 N^{4-2s} \int_0^t \|u(\tau)\|_s^2 e^{C_1(t-\tau)} d\tau \\
&\leq C_2 N^{4-2s} \|u\|_{Xs}^2 \int_0^t e^{C_1(t-\tau)} d\tau \\
&\leq C_2 N^{4-2s} \|u\|_{Xs}^2 \frac{e^{C_1 t} - 1}{C_1} \\
&\leq C_2 N^{4-2s} \|u\|_{Xs}^2 \frac{e^{C_1 T} - 1}{C_1} \\
&\leq C^2(T, \eta_1, \eta_2) N^{4-2s} \|u\|_{Xs}^2 \qquad \textbf{(3.15)}
\end{aligned}$$

for $s \geq 2$. Finally, we have

$$\|P_N u - u^N\|_{X_2} \leq C(T, \eta_1, \eta_2) \, N^{2-s} \|u\|_{Xs}^2. \qquad \textbf{(3.16)}$$

Using (3.4) and (3.16) in (3.3), we complete the proof of Theorem 2.

Corollary 2: Let $s \geq 2$ and $u(x,t)$ be the solution of the periodic initial value problem (2.1)-(2.2) satisfying $u(x,t) \in C^1([0,T]; H_p^s(\Omega))$ for any $T > 0$ and $u^N(x,t)$ be the solution of the semi-discrete scheme (3.1)-(3.2). There exists a constant C, independent of N, such that

$$\|u - u^N\|_2 \leq C(T, \eta_1, \eta_2) N^{2-s} \|u\|_{Xs}.$$

for the initial data $\phi, \psi \in H_p^s(\Omega)$.

3.3 The Fully-Discrete Scheme

We solve the HBq equation by combining a Fourier pseudo-spectral method for the space component and a fourth-order Runge Kutta scheme (RK4) for time. The MATLAB functions "fft" and "ifft" compute the discrete Fourier transform and its inverse for a function $f(x)$ by using an efficient Fast Fourier Transform at N equally spaced discrete points on $x \in [0, 2\pi]$. If the spatial period is normalized from $x \in [-L, L]$ to $X \in [0, 2\pi]$ using the transformation $X = \pi(x + L)/L$, the equation (3.1) becomes

$$u_{tt}^N - \left(\frac{\pi}{L}\right)^2 u_{XX}^N - \eta_1 \left(\frac{\pi}{L}\right)^2 u_{XXtt}^N + \eta_2 \left(\frac{\pi}{L}\right)^4 u_{XXXXtt}^N = \left(\frac{\pi}{L}\right)^2 (u^N)_{XX}^p. \qquad \textbf{(3.17)}$$

The interval $[0, 2\pi]$ is divided into N equal subintervals with grid spacing $\Delta X = 2\pi/N$, where the integer N is even. The spatial grid points are given by $X_j = 2\pi j/N$,

$j = 0,1,2,...,N$. The approximate solutions to $u^N(X_j,t)$ is denoted by $U_j(t)$. The discrete Fourier transform of the sequence $\{U_j\}$, i.e.

$$\widetilde{U}_k = \mathscr{F}_k[U_j] = \frac{1}{N}\sum_{j=0}^{N-1} U_j e^{-ikX_j}, \quad -N/2 \le k \le N/2-1 \tag{3.18}$$

gives the corresponding Fourier coefficients. Likewise, $\{U_j\}$ can be recovered from the Fourier coefficients by the inversion formula for the discrete Fourier transform (3.18), as follows:

$$U_j = \mathscr{F}_j^{-1}[\widetilde{U}_k] = \sum_{k=-\frac{N}{2}}^{\frac{N}{2}-1} \widetilde{U}_k e^{ikX_j}, \quad j = 0,1,2,...,N-1\ . \tag{3.19}$$

Here $\mathscr{F}$ denotes the discrete Fourier transform and $\mathscr{F}^{-1}$ its inverse. Applying the discrete Fourier transform to the equation (3.17) we get

$$(\widetilde{U}_k)_{tt} + \left(\frac{\pi k}{L}\right)^2 (\widetilde{U}_k) + \eta_1 \left(\frac{\pi k}{L}\right)^2 (\widetilde{U}_k)_{tt} + \eta_2 \left(\frac{\pi k}{L}\right)^4 (\widetilde{U}_k)_{tt} = -\left(\frac{\pi k}{L}\right)^2 (\widetilde{U}_k)^p. \tag{3.20}$$

This equation can be written as the following system

$$(\widetilde{U}_k)_t = \widetilde{V}_k, \tag{3.21}$$

$$(\widetilde{V}_k)_t = \kappa[\widetilde{U}_k + (\widetilde{U^p})_k] \tag{3.22}$$

where

$$\kappa = -\frac{(\pi k/L)^2}{1+\eta_1(\pi k/L)^2 + \eta_2(\pi k/L)^4}.$$

In order to handle the nonlinear term we use a pseudo-spectral approximation. That is, we use the formula $\mathscr{F}_k[(U_j)^p]$ to compute the k^{th} Fourier component of u^p. We use the fourth order Runge-Kutta method to solve the resulting ODE system (3.21)-(3.22) in time. The time interval $[0,T]$ is divided into M equal subintervals with temporal grid points $t_m = \frac{mT}{M}$. The value of the Fourier components at t_m is then denoted by $\widetilde{U}_k^m$. Using the RK4 method the solution of the ODE system (3.21)-(3.22) at time t_{m+1} is

$$\widetilde{U}_k^{m+1} = \widetilde{U}_k^m + \frac{\Delta t}{6}(g_{1,k}^m + 2g_{2,k}^m + 2g_{3,k}^m + g_{4,k}^m), \tag{3.23}$$

$$\widetilde{V}_k^{m+1} = \widetilde{V}_k^m + \frac{\Delta t}{6}(h_{1,k}^m + 2h_{2,k}^m + 2h_{3,k}^m + h_{4,k}^m), \tag{3.24}$$

where

$$
\begin{aligned}
g^m_{1,k} &= \widetilde{V}^m_k, \\
h^m_{1,k} &= \kappa[\widetilde{U}^m_k + (\widetilde{U^p})^m_k], \\
g^m_{2,k} &= \widetilde{V}^m_k + \frac{h^m_{1,k}}{2}, \\
h^m_{2,k} &= \kappa\{\mathscr{F}_k[(U^m_j + \mathscr{F}^{-1}_j[\frac{g^m_{1,k}}{2}])^p] + \widetilde{U}^m_k + \frac{g^m_{1,k}}{2}\}, \\
g^m_{3,k} &= \widetilde{V}^m_k + \frac{h^m_{2,k}}{2}, \\
h^m_{3,k} &= \kappa\{\mathscr{F}_k[(U^m_j + \mathscr{F}^{-1}_j[\frac{g^m_{2,k}}{2}])^p] + \widetilde{U}^m_k + \frac{g^m_{2,k}}{2}\}, \\
g^m_{4,k} &= \widetilde{V}^m_k + h^m_{3,k}, \\
h^m_{4,k} &= \kappa\{\mathscr{F}_k[(U^m_j + \mathscr{F}^{-1}_j[\frac{g^m_{3,k}}{2}])^p] + \widetilde{U}^m_k + g^m_{3,k}\}.
\end{aligned}
\tag{3.25}
$$

Finally, we find the approximate solution by using the inverse Fourier transform.

3.4 Numerical Experiments

The purpose of the present numerical experiments is to verify numerically that *(i)* the proposed Fourier pseudo-spectral scheme is highly accurate, *(ii)* the scheme exhibits the fourth-order convergence in time and *(iii)* the scheme has spectral accuracy in space. We will consider three test problems; propagation of a single solitary wave, collision of two solitary waves and blow-up of the solutions of higher-order Boussinesq equation. L_∞-error norm is defined as

$$
L_\infty\text{-error} = \max_i \mid u_i - U_i \mid \tag{3.26}
$$

where u_i denotes the exact solution at $u(X_i,t)$. As mentioned in the previous section we use fast Fourier transform (FFT) routines in Matlab (i.e. fft and ifft) to calculate Fourier transform and the inverse Fourier transform. As far as we know, there is no existing numerical study in the literature for the HBq equation. Therefore, we could not compare our numerical results with the results in the literature.

3.4.1 Propagation of a Single Solitary Wave

We study the single solitary wave solution of the HBq equation for $\eta_1 = \eta_2 = 1$. Therefore the initial conditions corresponding to the solitary wave solution (2.3) become as follows:

$$u(x,0) = A\,\mathrm{sech}^4(B\,x), \tag{3.27}$$

$$v(x,0) = 4AB\,c\,\mathrm{sech}^4(B\,x)\tanh(B\,x). \tag{3.28}$$

For $\eta_1 = \eta_2 = 1$ the solution represents a solitary wave initially at $x_0 = 0$ moving to the right with the amplitude $A \approx 0.39$, speed $c \approx 1.13$ and inverse width $B \approx 0.14$.

The problem is solved on the space interval $-100 \le x \le 100$ for times up to $T = 5$. We show the variation of L_∞-errors with N for the HBq equation for various power type nonlinearity, namely, $f(u) = u^p$ for $p = 2,3,4,5$ in Figure 3.1. The value of M is chosen to satisfy $\nu = \Delta t/\Delta x = 2.56 \times 10^{-3}$. We observe that the L_∞-errors decay as the number of grid points increases for various degrees of nonlinearity. Even in the case of the quintic nonlinearity, the L_∞-errors are about 10^{-12}. This experiment shows that the proposed method provides highly accurate numerical results even for the higher-order nonlinearities.

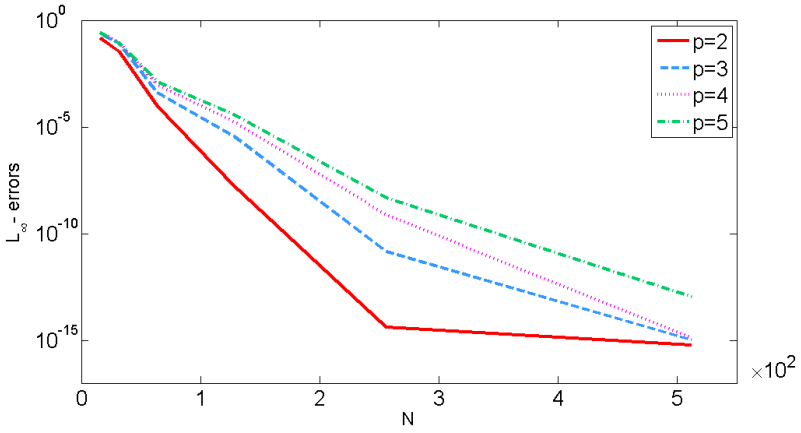

Figure 3.1: L_∞-errors for the increasing values of N

To validate whether the Fourier pseudo-spectral method exhibits the expected convergence rates in time we perform some numerical experiments for various values of M and a fixed value of N. In these experiments we take $N = 512$ to ensure that the error due to the spatial discretization is negligible. The convergence rates calculated from the L_∞-errors for the terminating time $T = 5$ are shown in Table 3.1. The computed convergence rates agree well with the fact that Fourier pseudo-spectral method exhibits the fourth order convergence in time.

Table 3.1: The convergence rates in time calculated from the L_∞-errors in the case of single solitary wave ($A \approx 0.39,\ \ N = 512$)

M	L_∞-error	Order
2	8.662E-3	-
5	2.530E-4	3.8561
10	1.614E-5	3.9704
50	2.623E-8	3.9903
100	1.637E-9	4.0021

To validate whether the Fourier pseudo-spectral method exhibits the expected convergence rate in space we now perform some further numerical experiments for various values of N and a fixed value of M. In these experiments we take $M = 1000$ to minimize the temporal errors. We present the L_∞-errors for the terminating time $T = 5$ together with the observed rates of convergence in Table 3.2.

Table 3.2: The convergence rates in space calculated from the L_∞-errors in the case of the single solitary wave ($A \approx 0.39,\ \ M = 1000$)

N	L_∞-error	Order
10	0.211E-1	-
50	1.747E-3	1.5480
100	4.431E-7	11.9450
150	6.500E-10	16.0916
200	3.884E-13	25.8017

These results show that the numerical solution obtained using the Fourier pseudo-spectral scheme converges rapidly to the accurate solution in space, which indicates exponential convergence.

3.4.2 Head-on Collision of Two Solitary Waves

In the second numerical experiment we study the collision of two solitary waves for the HBq equation with quadratic nonlinearity and various values of η_1 and η_2. The initial conditions are given by

$$\begin{aligned} u(x,0) &= A\,[\mathrm{sech}^4(B\,(x-40)) + \mathrm{sech}^4(B\,(x+40))], \\ v(x,0) &= 4A\,B\,c[\mathrm{sech}^4\,(B\,(x-40))\,\tanh\,(B\,(x-40)) \\ &\qquad -\mathrm{sech}^4\,(B\,(x+40))\,\tanh\,(B\,(x+40))]. \end{aligned}$$

We consider two solitary waves, one initially located at -40 and moving to the right with amplitude A ($c_1 > 0$) and one initially located at 40 and moving to the left with amplitude A ($c_2 = -c_1$). The magnitudes of the speed of two solitary waves are equal. The problem is solved again on the interval $-100 \leq x \leq 100$ for times up to $T = 72$ using the Fourier pseudo-spectral method. The experiments in this section are performed for $\Delta x = 0.4$ and $\Delta t = 10^{-2}$. Since the amplitude of the solitary waves depends on the choice of the parameters η_1 and η_2, we only consider the interaction of two solitary waves with the same amplitude.

Since an analytical solution is not available for the collision of two solitary waves, we cannot present the L_∞-errors for this experiment. But, as a numerical check of the proposed Fourier pseudo-spectral scheme, we present the evolution of the change in the conserved quantity $\mathscr{M}$ (mass) in the experiments.

In the first collision problem we consider the HBq equation for $\eta_1 = \eta_2 = 1$. The amplitude, the inverse width of both waves and the corresponding speed are $A \approx 0.39$, $B \approx 0.14$ and $\mid c \mid \approx 1.13$, respectively. We illustrate the surface plot of head-on collision of two solitary waves in Figure 3.2 and evolution of the change in the conserved quantity $\mathscr{M}$ (mass) in Figure 3.3.

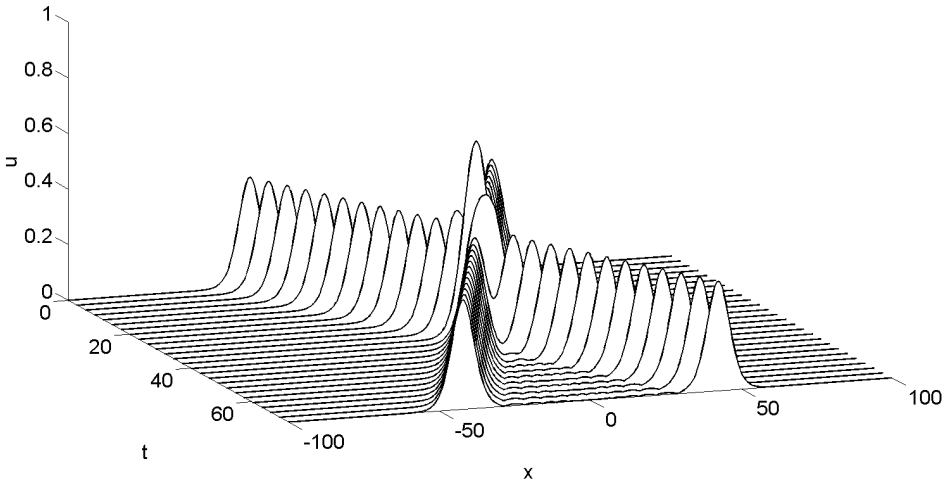

Figure 3.2: Head-on collision of two solitary waves with amplitude $A \approx 0.39$

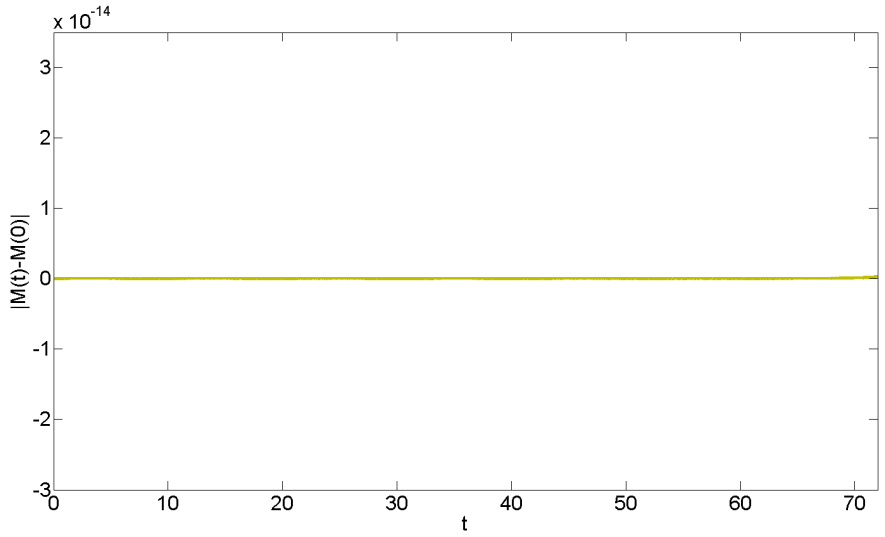

Figure 3.3: Evolution of the change in the conserved quantity mass

As can be seen from the Figure 3.3, the conserved quantity $\mathscr{M}$ (mass) remains constant in time and this behavior provides a valuable check on the numerical results.

In the second collision problem we consider the HBq equation for $\eta_1 = \eta_2 = 2$. The amplitude, the inverse width of both waves and the corresponding speed are $A \approx 1.08$, $B \approx 0.14$ and $\mid c \mid \approx 1.31$, respectively. We illustrate the surface plot of head-on collision of two solitary waves in Figure 3.4 and evolution of the numerical errors in the conserved quantity $\mathscr{M}$ (mass) in Figure 3.5.

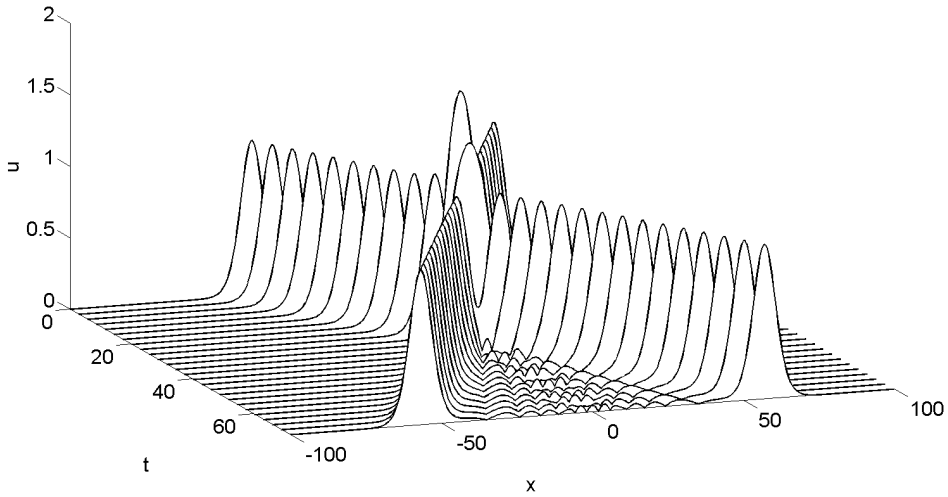

Figure 3.4: Head-on collision of two solitary waves with amplitude $A \approx 1.08$

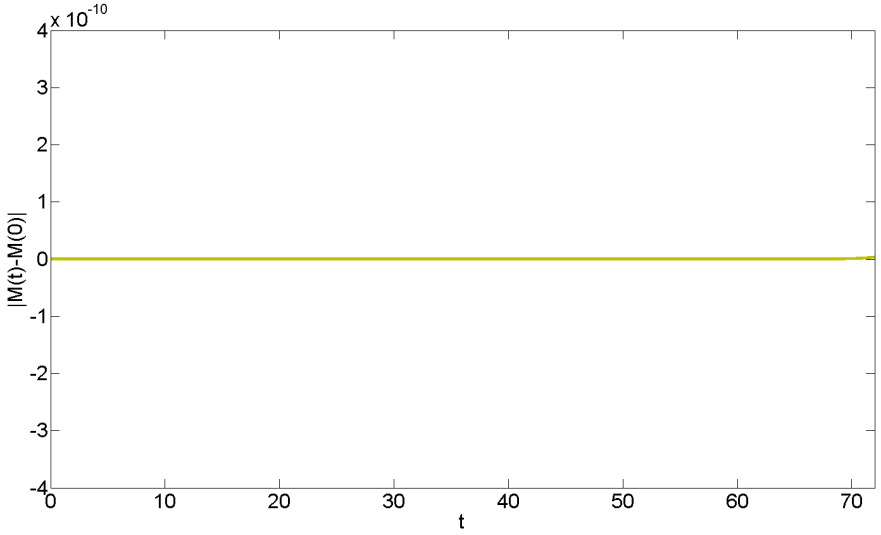

Figure 3.5: Evolution of the change in the conserved quantity mass

As we see our scheme conserves mass very well.

We see oscillating secondary waves in the Figure 3.4 unlike the Figure 3.2. Since the HBq equation cannot be solved by the inverse scattering method, the interaction of solitary waves are inelastic. Actually secondary waves exist in all nonlinear interactions, however they become more visible as we increase the amplitudes of the interacting waves. A general observation is that, as the degree of the nonlinearity increases, the waves become increasingly distorted after the interaction.

3.4.3 Blow-up

In this subsection, we test the ability of Fourier pseudo-spectral method to detect blow-up solutions of the HBq equation comparing the analytical blow-up results given in [11]. Throughout this section, we set the parameters $\eta_1 = \eta_2 = 1$ in (2.1). The HBq equation is one of the class of nonlocal equation studied in [11] with specific choice of the kernel function $\beta(x)$ with Fourier transform is

$$\widehat{\beta}(\xi) = \frac{1}{1+\eta_1\xi^2+\eta_2\xi^4} \ .$$

We refer to Theorem 5.2 in [11] as the blow-up criteria. This theorem can be restated for the HBq equation as:

Theorem 3 [11] : Suppose $\phi = \Phi_x, \psi = \Psi_x$ for some $\Phi, \Psi \in H^2(\Omega)$. If there is some $\mu > 0$ such that

$$pf(p) \leq 2(1+2\mu)F(p) \quad \text{for all } p \in \mathbb{R}, \tag{3.29}$$

and $\mathscr{E}(0) < 0$, then the solution u of the Cauchy problem for HBq equation with the initial condition $u(x,0) = \phi(x)$, $u_t(x,0) = \psi(x)$ blows up in finite time.

In our experiments, we generalized the blow-up results in [12], where the author discusses the blow-up solutions for the generalized improved Boussinesq equation.

We consider the blow-up solutions for both the quadratic and cubic nonlinearities.
In the first experiment, we study the HBq equation with quadratic nonlinearity. The initial conditions are given by

$$\begin{aligned} \phi(x) &= a(\frac{2x^2}{3}-1)e^{-\frac{x^2}{3}}, \\ \psi(x) &= \left(x^2-1\right)e^{-\frac{x^2}{3}}. \end{aligned} \tag{3.30}$$

To satisfy the blow-up conditions $\mathscr{E}(0) < 0$ we choose $a = 4$, then the condition (3.29) is also satisfied for $\mu = \frac{1}{4}$. The problem is solved on the interval $-10 \leq x \leq 10$ for times up to $T = 4$. We present the variation of the L_∞ norm of the approximate solution obtained using the Fourier pseudo-spectral scheme for $N = 64$ and $M = 400$ in Figure 3.6. We point out that the initial amplitude is 4 in the initial condition given by equation (3.30). However, the amplitude of the numerical solution increases as time increases

and it becomes approximately 10^{94} near the numerical blow-up time. The numerical results strongly indicate that a blow-up is well underway by time $t^* = 3.8$.

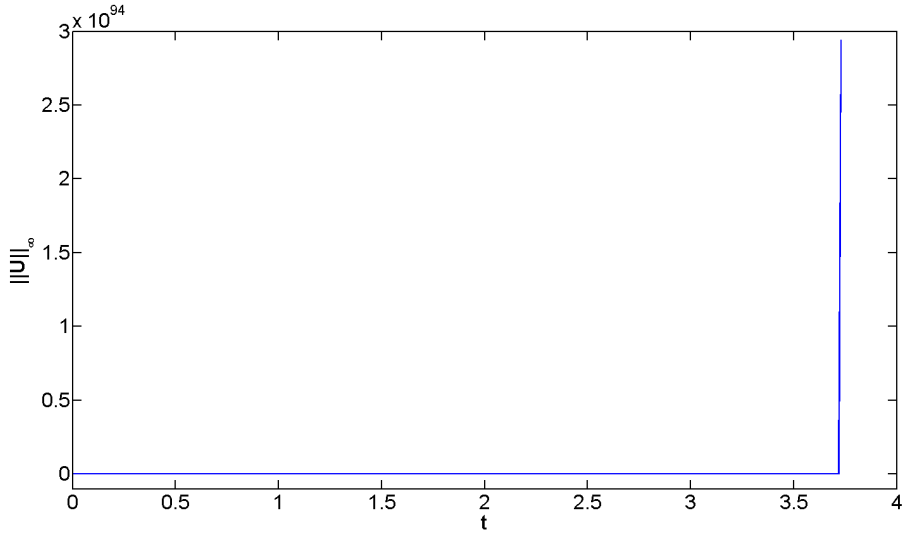

Figure 3.6: The variation of $\| U \|_\infty$ with time

In order to see increasing $\| U \|_\infty$ with time clearly, we focus on the smaller interval in Figure 3.7.

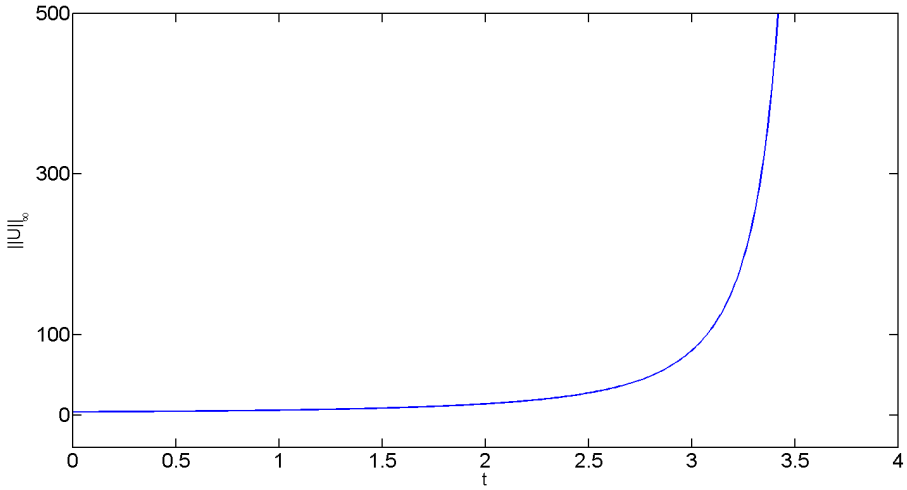

Figure 3.7: The variation of $\| U \|_\infty$ with time

In the second experiment, we consider the HBq equation with cubic nonlinearity. We consider the following initial conditions

$$\phi(x) = a(\frac{x^2}{2} - 1)e^{-\frac{x^2}{4}},$$
$$\psi(x) = \left(1 - x^2\right) e^{-\frac{x^2}{2}}. \tag{3.31}$$

To satisfy the blow-up condition $\mathscr{E}(0) < 0$ we choose $a = 13$, then the condition (3.29) is also satisfied for $\mu = \frac{1}{2}$. The problem is solved on the interval $-10 \leq x \leq 10$ for times up to $T = 0.4$. We present the variation of the L_∞ norm of the approximate solution for $N = 64$ and $M = 40$ in Figure 3.8. The amplitude of the numerical solution increases as time increases. The numerical results strongly indicate that a blow-up is well underway by the time $t^* = 0.36$.

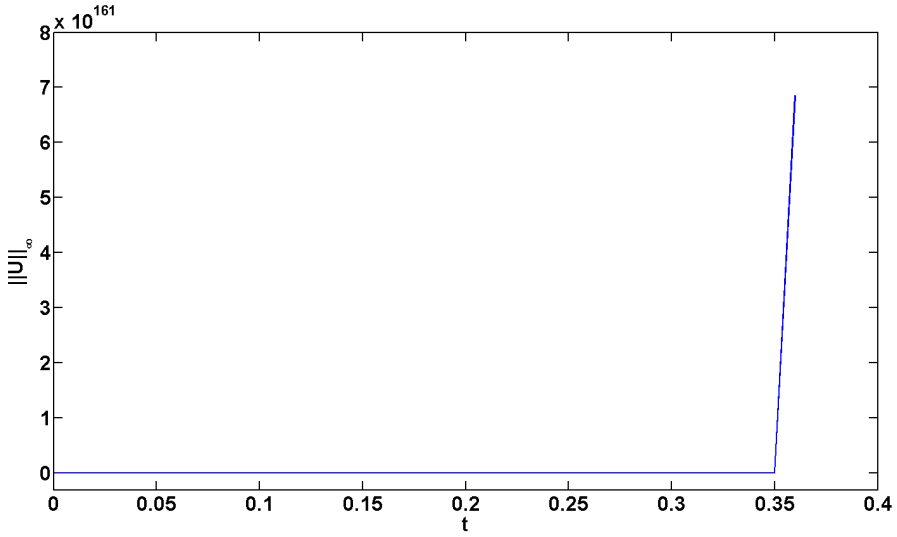

Figure 3.8: The variation of $\| U \|_\infty$ with time

In order to see increasing of the $\| U \|_\infty$ with time clearly, we focus on the smaller interval in Figure 3.9.

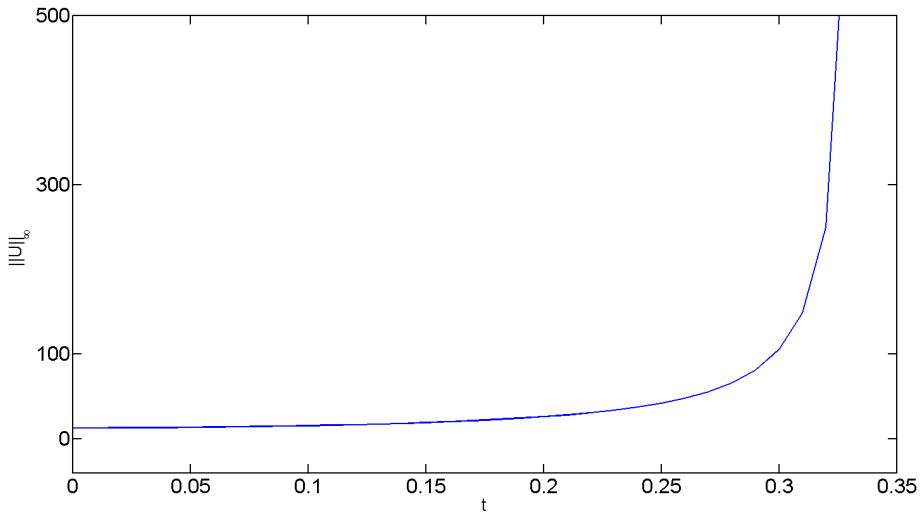

Figure 3.9: The variation of $\| U \|_\infty$ with time

3.4.4 Conclusion

As a conclusion, we sum up that i) the Fourier pseudo-spectral method has been presented for the HBq equation, ii) proposed scheme provides fourth order convergence in time and exponential convergence in space, iii) the Fourier pseudo-spectral method provides highly accurate results for various type of nonlinearities, iv) the method is very successful to simulate the propagation of the single solitary wave and the collision of solitary waves, v) the method does not miss the blow-up phenomena.

REFERENCES

[1] **Canuto, C.**, **Hussaini, M.Y.**, **Quarteroni, A. and Zang, T.A.** (1988). *Spectral Methods in Fluid Dynamics*, Springer-Verlag, Berlin Heidelberg.

[2] **Evans, L.C.** (1998). *Partial Differential Equations*, Providence Rhode Land: American Mathematical Society, United States of America.

[3] **Kreiss, H.O. and Oliger, J.** (1979). Stability of the Fourier method, *SIAM J. Numer. Anal.*, ***16***, 421–433.

[4] **Rosenau, P.** (1987). Dynamics of dense lattices, *Phys. Rev. B*, ***36***, 5868–5876.

[5] **Schneider, G. and Wayne, C.E.** (2001). Kawahara dynamics in dispersive media, *Physica D: Nonlinear Phenomena*, ***152-153***, 384–394.

[6] **Duruk, N.**, **Erkip, A. and Erbay, H.A.** (2009). A higher-order Boussinesq equation in locally non-linear theory of one-dimensional non-local elasticity, *IMA J. Appl. Math.*, ***74***, 97–106.

[7] **Duruk, N.**, (2006), Cauchy Problem for a Higher-Order Boussinesq Equation, MSc. Dissertation, SabancıUniversity Graduate School of Engineering and Natural Science, Mathematics Graduate Program, Istanbul, Turkey.

[8] **Canuto, C. and Quarteroni, A.** (1982). Approximation results for orthogonal polynomials in Sobolev Spaces, *Mathematics of Computation*, ***38***, 67–86.

[9] **Rashid, A. and Akram, S.** (2010). Convergence of Fourier spectral method for resonant long-short nonlinear wave interaction, *Applications of Mathematics*, ***55***, 337–350.

[10] **Runst, T. and Sickel, W.** (1996). *Sobolev spaces of fractional order, Nemytskij operators, and nonlinear partial differential equations*, volume 3, Walter de Gruyter.

[11] **Duruk, N.**, **Erbay, H.A. and Erkip, A.** (2010). Global existence and blow-up for a class of nonlocal nonlinear Cauchy problems arising in elasticity, *Nonlinearity*, ***23***, 107–118.

[12] **Godefroy, A.** (1998). Blow-up solutions of a generalized Boussinesq equation, *IMA J. Numer. Anal.*, ***60***, 122–138.

CURRICULUM VITAE

Name Surname: Göksu TOPKARCI

Place and Date of Birth: Istanbul, 05.01.1989

Adress: İstanbul Teknik Üniversitesi Fen-Edebiyat Fakültesi Matematik Bölümü
Maslak İstanbul/TÜRKİYE

E-Mail: topkarci@itu.edu.tr

B.Sc.: Major on Mathematical Engineering (2012), ITU

Professional Experience and Rewards:

High Honor List at graduation.
Research Assistant at Istanbul Technical University.

List of Publications and Presentations on the Thesis:

- **Topkarcı, G.**, Muslu, G. M. and Borluk, H., "An efficient and accurate numerical method for the higher order Boussinesq equation."(Submitted)
- **Topkarcı, G.**, Borluk, H. and Muslu, G. M., "The higher-order Boussinesq equation with periodic boundary conditions", *Book of abstracts: SIAM Nonlinear Waves and Coherent Structures (SIAM NW14)*, p. 70, Cambridge, 2014.
- **Topkarcı, G.**, Borluk, H. and Muslu, G. M., "A Fourier pseudo-spectral method for the higher-order Boussinesq equation", *Abstracts of Contributed Talks: BMS Summer School 2014 Applied Analysis for Materials*, p. 5, Berlin, 2014.